


Harmonically Confined Particles with Long-Range Repulsive Interactions

S. Agarwal,^{1,2} A. Dhar,¹ M. Kulkarni,¹ A. Kundu,¹ S. N. Majumdar,³ D. Mukamel,⁴ and G. Schehr³
¹*International Centre for Theoretical Sciences, Tata Institute of Fundamental Research, Bengaluru 560089, India*
²*Birla Institute of Technology and Science, Pilani 333031, India*
³*LPTMS, CNRS, Univ. Paris-Sud, Université Paris-Saclay, 91405 Orsay, France*
⁴*Department of Physics of Complex Systems, Weizmann Institute of Science, Rehovot 7610001, Israel*

 (Received 11 June 2019; published 6 September 2019)

We study an interacting system of N classical particles on a line at thermal equilibrium. The particles are confined by a harmonic trap and repel each other via pairwise interaction potential that behaves as a power law $\propto \sum_{i \neq j}^N |x_i - x_j|^{-k}$ (with $k > -2$) of their mutual distance. This is a generalization of the well-known cases of the one-component plasma ($k = -1$), Dyson's log gas ($k \rightarrow 0^+$), and the Calogero-Moser model ($k = 2$). Because of the competition between harmonic confinement and pairwise repulsion, the particles spread over a finite region of space for all $k > -2$. We compute exactly the average density profile for large N for all $k > -2$ and show that while it is independent of temperature for sufficiently low temperature, it has a rich and nontrivial dependence on k with distinct behavior for $-2 < k < 1$, $k > 1$ and $k = 1$.

DOI: 10.1103/PhysRevLett.123.100603

Introduction.—A gas of N classical particles, confined by a harmonic potential on a line and interacting with each other via pairwise repulsion, constitutes one of the simplest interacting particle systems that has been well studied in the past. It has seen a recent revival in the wake of the physics of cold atoms. When the pairwise repulsive interaction decays as a power law of the distance between the particles, the energy of the so-called Riesz gas [1] is given by

$$E(\{x_i\}) = \frac{1}{2} \sum_{i=1}^N x_i^2 + \frac{J \operatorname{sgn}(k)}{2} \sum_{i \neq j} \frac{1}{|x_i - x_j|^k}, \quad (1)$$

where $J > 0$ and $\{x_i\}$ ($i = 1, 2, \dots, N$) denote the positions of the particles on the line. The index $k > -2$ characterizes the strength of the pairwise interaction and $\operatorname{sgn}(k)$ in the prefactor ensures a repulsive interaction. For $k < -2$, the quadratic potential is not strong enough to counter the strong repulsion and confine the particles. Consequently the particles fly off to $\pm\infty$ and thus the case $k < -2$ is not physically interesting. Given the energy in (1), the joint probability distribution function (PDF) of the particles' positions is given by the Boltzmann weight, $P(x_1, \dots, x_N) = e^{-\beta E(\{x_i\})} / Z_N(\beta)$, where β is the inverse temperature ($k_B = 1$) and $Z_N(\beta) = \int \prod_{i=1}^N dx_i e^{-\beta E(\{x_i\})}$ is the normalizing partition function. The harmonic potential tries to confine the particles near the center of the trap, while the repulsive interaction tries to push them apart. As a result of the competition between the two terms, it turns out that the particles get confined to a finite region of space for large N , with a space-dependent

average macroscopic density, $\langle \rho_N(x) \rangle = N^{-1} \sum_{i=1}^N \langle \delta(x - x_i) \rangle$ (normalized to unity), where $\langle \dots \rangle$ denotes an average with respect to the Boltzmann weight. A basic natural question is as follows: what is the configuration of x_i 's that minimizes the energy in (1) for large N and what is the density profile in the ground state? This is a classic and important optimization problem both in physics (see below) and in mathematics (see, e.g., Refs. [2–4]) whose solution, for generic $k > -2$, is hitherto unknown. A related question is as follows: how does the average density profile depend on the inverse temperature β ?

This problem is of great general interest as there are varied physical systems that correspond to special values of k . We start with $k = -1$ where the interaction is linearly repulsive with distance. This is the well-known one-dimensional one-component plasma (1D OCP) [5], consisting of oppositely charged particles with pairwise Coulomb interaction (linear in 1D) and overall charge neutrality [6–10]. Integrating out the positions of the negative charges gives rise to an effective quadratic confinement for the positive charges and the effective energy of the N positive charges with coordinates $\{x_i\}$ is precisely given by (1) with $k = -1$. In this case, the energy can be easily minimized by ordering the positions of the particles leading to an equispaced configuration [6–10]. Moreover, for large N , the average density profile $\langle \rho_N(x) \rangle$ turns out to be independent of β and approaches a scaling form $\langle \rho_N(x) \rangle \rightarrow (1/N) \tilde{\rho}_{\text{OCP}}(x/N)$, where the scaled density $\tilde{\rho}_{\text{OCP}}(y) = 1/(2J)$ is uniform over the interval $[-J, +J]$ and vanishes outside [3,6–11].

The second and perhaps the most well-studied example corresponds to the limit $k \rightarrow 0^+$, where we replace $\operatorname{sgn}(k)$ in Eq. (1) by $+1$, use $|x_i - x_j|^{-k} \approx 1 - k \log |x_i - x_j|$, and

set $J = 1/k$. The energy in (1) then reduces, up to an overall additive constant, to

$$E[\{x_i\}] = \frac{1}{2} \sum_{i=1}^N x_i^2 - \frac{1}{2} \sum_{i \neq j} \ln |x_i - x_j|. \quad (2)$$

This is the celebrated log-gas of Dyson [12]. For the special values of $\beta = 1, 2$, and 4 , the Boltzmann weight of the Dyson's log gas $P(\{x_i\}) = \{1/[Z_N(\beta)]\} \exp[-\beta E[\{x_i\}]]$ can be identified with the joint distribution of N real eigenvalues of an $N \times N$ matrix belonging to the Gaussian ensembles of the random matrix theory (RMT): respectively Gaussian orthogonal ensemble, Gaussian unitary ensemble, and Gaussian symplectic ensemble [5,13]. Gaussian ensembles are the cornerstones of RMT with myriad of applications, ranging from nuclear physics, mesoscopic transport, quantum chaos, and number theory all the way to finance and big-data science [5,13–15]. The Dyson's log gas with arbitrary $\beta > 0$ also appears in RMT as the joint PDF of the eigenvalues of the so-called Dumitriu-Edelman β -ensemble of tridiagonal random matrices [16]. The average density for large N converges to the scaling form, independently of β ,

$$\langle \rho_N(x) \rangle \approx \frac{1}{\sqrt{N}} \tilde{\rho}_{\text{sc}} \left(\frac{x}{\sqrt{N}} \right), \quad \tilde{\rho}_{\text{sc}}(y) = \frac{1}{\pi} \sqrt{2 - y^2}. \quad (3)$$

Thus the scaled density is supported over $[-\sqrt{2}, +\sqrt{2}]$ and is known as the celebrated Wigner semicircular law [17]. This central result of RMT has been instrumental in understanding the global properties in a variety of systems including growth models in $1 + 1$ dimensions belonging to the Kardar-Parisi-Zhang universality class [18], noninteracting trapped fermions [19–21] where the Wigner semicircle can also be obtained from the so-called local density approximation [22], nonintersecting Brownian motions [23–25], graph theory, and communication networks [14].

The third physical example corresponds to $k = 2$, i.e., with inverse-square repulsion. For $k = 2$, (1) is the celebrated Calogero-Moser model [26–29], which is integrable and is ubiquitous in diverse fields [30]. Curiously, it turns out that for any finite N , in the minimum energy configuration of both the Dyson's log gas ($k \rightarrow 0^+$) and the Calogero-Moser model ($k = 2$), the particle positions x_i 's coincide exactly [31,32] with the N zeros of the Hermite polynomial of degree N . Consequently, for large N , the scaled average density for $k = 2$ also approaches the Wigner semicircular law in Eq. (3) and as in the Dyson's log gas case, the semicircular law is independent of β . This is rather strange: even though the long-range repulsive interaction in the Dyson's log gas is much stronger than that of the inverse-square gas, the average density profile is identical in the two cases. This raises a very interesting and natural question: How does the shape of the average scaled density for large N vary as one tunes the parameter k ? The

appearance of the semicircular law both for $k \rightarrow 0^+$ and $k = 2$ suggests an intriguing possibility of a “nonmonotonic” dependence of the shape of the average density as one tunes up k . This question on the dependence of the average density on k also has practical implications in a number of physical contexts. For example, in a typical cold atom experimental setup, a quadratic confining potential is natural due to the usage of optical laser traps. In addition, it is possible to induce long-range power-law repulsive interactions between such atoms. For instance, charged particles interacting via the 3D Coulomb repulsion, but confined to a line by highly anisotropic optical trap, would correspond to $k = 1$. Similarly, $k = 3$ describes a dipolar gas confined to 1D [33–35]. For $k \rightarrow \infty$, the Riesz gas reduces to a truly short-ranged repulsive gas similar to the harmonically confined screened Coulomb or Yukawa gas studied in Refs. [11,36]. In addition, other values of k have either been realized in experimental setups or could potentially be realized [37].

In this Letter, we address this interesting question of the dependence of the average density on k and obtain exact results for large N . We show that for large N the average density is independent of β for all k (for sufficiently large β) [38], but has a rich and nontrivial dependence on k . On general grounds the average density is expected to have a scaling form $\langle \rho_N(x) \rangle \approx N^{-\alpha_k} \tilde{\rho}_k(x/N^{\alpha_k})$ for large N , where N^{α_k} corresponds to the typical scale of the position of the particles in the trap. Indeed, we do find this behavior, but with a twist. We show that there is a drastic change of behavior of the exponent α_k as well as the scaling function $\tilde{\rho}_k(y)$ at $k = 1$. For the exponent, we get

$$\alpha_k = \begin{cases} \frac{1}{k+2}, & -2 < k < 1 \\ \frac{k}{k+2}, & k > 1. \end{cases} \quad (4)$$

The scaling function $\tilde{\rho}_k(y)$ has a support over $[-\ell_k/2, +\ell_k/2]$ and can be expressed as $\tilde{\rho}_k(y) = \ell_k^{-1} F_k(y/\ell_k)$, where $F_k(z)$ is given by

$$F_k(z) = \frac{1}{B(\gamma_k + 1, \gamma_k + 1)} \left(\frac{1}{4} - z^2 \right)^{\gamma_k}, \quad (5)$$

with $-1/2 \leq z \leq 1/2$, and $B(a, b)$ is the standard Beta function. Thus the density either diverges or vanishes at the two scaled edges $z = \pm 1/2$ with an exponent γ_k , which also exhibits a change of behavior at $k = 1$, namely,

$$\gamma_k = \begin{cases} \frac{k+1}{2}, & -2 < k < 1 \\ \frac{1}{k}, & k > 1. \end{cases} \quad (6)$$

The support length ℓ_k is nonuniversal and depends explicitly on k and the coupling strength J (for the exact expressions of ℓ_k , see Eqs. (36) and (65) of Supplemental Material [45]). The scaling function $F_k(z)$ depends only on

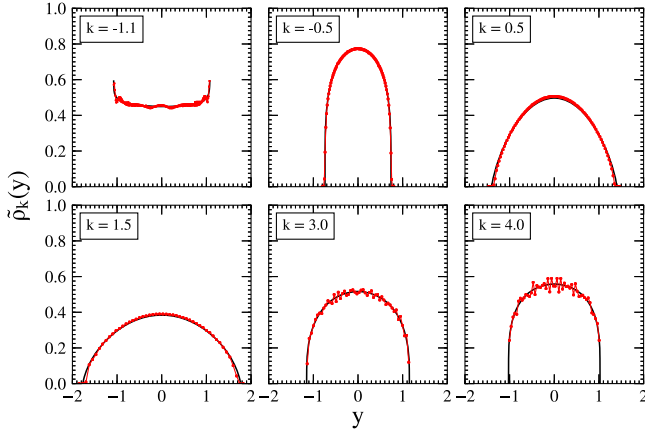


FIG. 1. The numerical (MC) average scaled density $\tilde{\rho}_k(y)$ vs y (red dots) for different values of k : for $-2 < k < 1$ in the top three panels and for $k > 1$ in the bottom three panels (where $N = 200$ and $\beta = 2$). The numerical curves are compared to analytical predictions (black) with excellent agreement. Oscillations are somewhat prominent at higher $|k|$ due to the finite N effects. The ensemble average is over 2×10^8 MC samples.

k , and is independent of β and J . The case $k = 1$ is marginal with additional logarithmic corrections (we discuss this later). We show that this change of behavior at $k = 1$ can be traced back to the fact that, for $k < 1$, the large distance behavior of the interaction term controls the large N behavior of the density. In contrast, for $k > 1$, the limiting density is determined by the short distance behavior of the interaction term. This gives rise to an effective field theory that is fundamentally different for $k < 1$ and $k > 1$. Thus $k \rightarrow 0^+$ (Dyson's log gas) and $k = 2$ (inverse-square gas) share the same average density profile, but the physics is rather different in the two cases. For $k \rightarrow -1$, we recover the flat density of the 1D OCP. Also, in the limit $k \rightarrow \infty$ we again get a flat density, consistent with the results for the 1D harmonically confined Yukawa gas [11,36]. We also performed Monte Carlo (MC) simulations for several values of k , finding excellent agreement with our analytical predictions (see Fig. 1).

Regime 1: $-2 < k < 1$.—Assuming both terms in the energy (1) are of the same order for large N , the energy scale can be estimated as follows. Let the typical position of a particle scale as $x_{\text{typ}} \sim N^{\alpha_k}$ for large N , where α_k is to be determined. Then the first term in (1) scales as $\sim N^{2\alpha_k+1}$, while the second term [where the double sum contains typically $N(N-1) \approx N^2$ terms] scales as $\sim JN^{2-k\alpha_k}$. Demanding they are of the same order fixes the exponent $\alpha_k = 1/(k+2)$ [see the first line in Eq. (4)]. Hence the total energy scales as $E \sim N^{2\alpha_k+1} \sim N^{(4+k)/(2+k)}$ in this regime. To find the configuration that dominates the partition function $Z_N(\beta)$ for large N , we generalize the method used for the Dyson's log gas ($k \rightarrow 0^+$ limit) [12, 48–50]. It turns out to be convenient to express the coarse-grained energy in terms of a macroscopic density $\rho_N(x)$ and

use the relation $\sum_{i=1}^N f(x_i) \approx N \int f(x) \rho_N(x) dx$, valid for any smooth function $f(x)$. Next, we rescale $x = N^{\alpha_k} y$ with $y \sim O(1)$. Under this rescaling, the density transforms as $\rho_N(x) \approx N^{-\alpha_k} \tilde{\rho}_k(y = xN^{-\alpha_k})$, where we assume $\tilde{\rho}_k(y)$ is smooth and normalizable, $\int \tilde{\rho}_k(y) dy = 1$. Consequently, the coarse-grained partition function for large N can be expressed as a functional integral over the density field $\tilde{\rho}_k(y)$ (for details see Supplemental Material [45]),

$$Z_N(\beta) \sim \int d\mu \int \mathcal{D}[\tilde{\rho}_k] \exp(-\beta N^{\frac{4+k}{2+k}} \Sigma[\tilde{\rho}_k(y)]), \quad (7)$$

where the action $\Sigma[\tilde{\rho}_k(y)]$ is given by (see also Ref. [51] for a rigorous proof in the cases $0 < k < 1$)

$$\Sigma[\tilde{\rho}_k(y)] = \frac{J \text{sgn}(k)}{2} \int dy \int dy' \frac{\tilde{\rho}_k(y) \tilde{\rho}_k(y')}{|y - y'|^k} + \frac{1}{2} \int dy y^2 \tilde{\rho}_k(y) - \mu \left(\int dy \tilde{\rho}_k(y) - 1 \right). \quad (8)$$

Here μ is the Lagrange multiplier that enforces the constraint $\int \tilde{\rho}_k(y) dy = 1$. Note that in the integrand of Eq. (7), we have only kept the leading order contributions to the energy. Both the entropy term (generated in going from microscopic configurations to the macroscopic density) as well as the short distance behavior of the interaction energy have been neglected, as they are of lower order in N for $-2 < k < 1$. This is valid as long as $\beta \gg N^{-2\alpha_k}$ where $\alpha_k = 1/(k+2)$ [38,45]. Thus the effective action $\Sigma[\tilde{\rho}_k(y)]$ is manifestly *nonlocal* reflecting the long-range nature of the repulsive interaction. We see later that this nonlocality manifests only for $-2 < k < 1$. For large N , the partition function in Eq. (7) can then be evaluated by the saddle point method. Minimizing the action $\Sigma[\tilde{\rho}_k(y)]$ in (8) with respect to $\tilde{\rho}_k(y)$ gives the saddle point equation for the optimal density

$$\frac{y^2}{2} + J \text{sgn}(k) \int dy' \frac{\tilde{\rho}_k(y')}{|y' - y|^k} = \mu. \quad (9)$$

This equation is valid over the support of $\tilde{\rho}_k(y)$. The density is clearly symmetric in y ; hence the support is over $[-\ell_k/2, \ell_k/2]$, where ℓ_k is fixed using the normalization $\int_{-\ell_k/2}^{\ell_k/2} \rho_k(y) dy = 1$. Taking a further derivative of (9) with respect to y leads to a singular integral equation

$$\text{PV} \int_{-\ell_k/2}^{\ell_k/2} \frac{\text{sgn}(y' - y)}{|y - y'|^{k+1}} \tilde{\rho}_k(y') dy' = -\frac{y}{J|k|}, \quad k \neq 0, \quad (10)$$

where PV denotes the principal value, which needs to be taken only for $k > 0$. Also, for $k \rightarrow 0$, J has to be rescaled such that $J|k| = 1$. Solving this singular integral equation poses the main technical challenge. Fortunately, it turns out that for $-2 < k < 1$, this equation can be transformed into the well-studied Sonin form [52–58], and can subsequently

be inverted to obtain $\tilde{\rho}_k(y)$ explicitly [45]. We then obtain the exact saddle point density $\tilde{\rho}_k(y) = \ell_k^{-1} F_k(y/\ell_k)$, where ℓ_k is given in Supplemental Material [45] and $F_k(z)$ is given in Eq. (5) with $\gamma_k = (k+1)/2$. Note that the Sonin inversion formula also indicates that there is no physical solution (saddle point density) for $k > 1$. Hence, this solution is valid only in the range $-2 < k < 1$. Furthermore, since β appears only in the factor $\beta N^{(4+k)/(2+k)}$ outside the action $\Sigma[\tilde{\rho}_k(y)]$ in (7), it is clear that the saddle point density is independent of β : large N is equivalent to large β . In addition, the average density $\langle \rho_N(x) \rangle$, for large N , clearly coincides with the saddle point density as the average over all possible densities is dominated by the saddle point. In Fig. 1, upper panels, we compare our theoretical predictions with MC simulations for three representative values of k in the range $-2 < k < 1$ and find excellent agreement. Note that in the range $-2 < k < -1$ the density diverges at the edges $\pm \ell_k/2$, while for $-1 < k < 1$ the density vanishes at the edges. Exactly at $k = -1$, the density is flat, consistent with the 1D OCP result.

Regime 2: $k \geq 1$.—It turns out that, for $k > 1$, the interaction term in (1) containing the double sum is dominated by particles that are very close to each other, i.e., almost nearest neighbors. As a result, the short distance properties of the interaction term play a more dominant role compared with their long distance behavior. This leads to an effective field theory that is local in the density and is much simpler. To compute the effective coarse-grained energy for large N , we then take a different path than the $k < 1$ case (for details see Supplemental Material [45]). First, it is convenient to order the particle positions so that x_i increases with the label i [this is fine since the energy (1) is invariant under permutation of labels]. We then replace the discrete particle label i by a continuous coordinate and the position x_i is approximated by a smooth continuous function $x(i)$. Next, we approximate $x_i - x_j \approx (i-j)x'(i)$ where $x'(i) = dx(i)/di$ and we have kept only the first term in the Taylor expansion anticipating that it captures the leading short distance behavior. Our next step is to express $x'(i)$ in terms of the local smooth macroscopic density $\rho_N(x)$ (normalized to unity). In fact, the local slope of the smooth function $x(i)$, i.e., $x'(i) > 0$ is simply the inverse of the number density $N\rho_N(x)$, i.e., $x'(i) = 1/[N\rho_N(x)]$. Thus the double sum in (1) can be approximated, to leading order for large N , by $\sum_{i \neq j} |x_i - x_j|^{-k} = \sum_{i \neq j} |i-j|^{-k} [N\rho_N(x_i)]^k$. The sum over j , for fixed i , is convergent for all $k > 1$ and simply gives a factor $2\zeta(k)$, where $\zeta(k) = \sum_{n=1}^{\infty} n^{-k}$ is the Riemann zeta function. Furthermore, the sum over i can be replaced by an integral using the relation $\sum_{i=1}^N f(x_i) \approx N \int f(x) \rho_N(x) dx$ mentioned before. Using this relation in both terms of (1) leads to a coarse-grained energy $\mathcal{E} \equiv \mathcal{E}[\rho_N(x)]$ [45],

$$\mathcal{E} \approx \frac{N}{2} \int dx x^2 \rho_N(x) + J\zeta(k) N^{k+1} \int dx [\rho_N(x)]^{k+1}, \quad (11)$$

which is completely local in the density $\rho_N(x)$, unlike (8) for $-2 < k < 1$ that involved densities at two space-separated points. We then rescale $x \rightarrow xN^{-\alpha_k}$ and write $\rho_N(x) = N^{-\alpha_k} \tilde{\rho}_k(y = xN^{-\alpha_k})$. It is easy to see that for both terms in (11) to be of the same order in N for large N , we need to choose $\alpha_k = k/(k+2)$, as stated in the second line of (4). Hence, the total energy scales as $E \sim N^{[(3k+2)/(k+2)]}$ for large N . The coarse-grained partition function $Z_N(\beta)$ can then be written as

$$Z_N(\beta) \sim \int d\mu \int \mathcal{D}[\tilde{\rho}_k] \exp(-\beta N^{\frac{3k+2}{k+2}} \Sigma[\tilde{\rho}_k(y)]), \quad (12)$$

where the action $\Sigma[\tilde{\rho}_k(y)]$ is given by

$$\begin{aligned} \Sigma[\tilde{\rho}_k(y)] = & \frac{1}{2} \int dy y^2 \tilde{\rho}_k(y) + J\zeta(k) \int dy [\tilde{\rho}_k(y)]^{k+1} \\ & - \mu \left(\int dy \tilde{\rho}_k(y) - 1 \right), \end{aligned} \quad (13)$$

with μ again denoting the Lagrange multiplier enforcing the normalization of the density. Note that we have kept the leading order contribution for large N in the integrand in (12) and again neglected the entropy as well as subdominant singular terms that are of lower order in N . For large N , the integral (12) can again be evaluated by the saddle point method. Minimizing the action gives the saddle point equation

$$\frac{1}{2} y^2 + J\zeta(k)(k+1)[\tilde{\rho}_k(y)]^k = \mu. \quad (14)$$

Trivially solving this equation gives $\tilde{\rho}_k(y) = (1/\ell_k) F_k(y/\ell_k)$, with support over $[-\ell_k/2, \ell_k/2]$, where $\ell_k = 2\sqrt{2\mu}$ is fixed from the normalization and is given explicitly in Supplemental Material [45]. The scaling function $F_k(z)$ is then of the form in (5) with the exponent $\gamma_k = 1/k$. The saddle point density coincides with the average density $\langle \rho_N(x) \rangle$ for large N . In addition, since β appears only in the combination $\beta N^{(3k+2)/(k+2)}$ outside the action in (12), clearly the saddle point density and hence the average density $\langle \rho_N(x) \rangle$ is independent of β for large N , as long as $\beta \gg N^{-2\alpha_k}$ where $\alpha_k = k/(k+2)$ [38,45]. This analytical prediction is then verified in MC simulations (see the bottom panels in Fig. 1).

The marginal case $k = 1$ lies at the borderline between regime 1 and regime 2. In this case, one would expect logarithmic corrections. Indeed, we find [45] that the average density approaches a scaling form, $\langle \rho_N(x) \rangle \sim L_N^{-1} \tilde{\rho}_1(x/L_N)$, where the typical position of a particle scales as $L_N \approx (N \ln N)^{1/3}$ for large N . The scaling function $\tilde{\rho}_1(y)$ is supported over $[-\ell_1/2, \ell_1/2]$ with $\ell_1 = 2\sqrt{2\mu}$ and is given by

$$\tilde{\rho}_1(y) = \frac{1}{4J} (2\mu - y^2), \quad \mu = \frac{1}{2} (3J)^{2/3}. \quad (15)$$

This can be also cast in the scaling form $\tilde{\rho}_1(y) = (1/\ell_1)F_1(y/\ell_1)$, where $F_1(z)$ is given in (5) with $\gamma_1 = 1$. Numerical simulations are in good agreement with our analytical prediction, as shown in Supplemental Material [45].

Conclusions.—In this Letter, we have computed analytically the average density profile of a classical gas of harmonically confined particles that repel each other with the repulsive interaction behaving as a power law with exponent $-k$ of the distance between any pair of particles. Our result generalizes in a nontrivial way, to arbitrary $k > -2$, the three famous classical examples: the 1D OCP ($k = -1$), the Dyson’s log gas in RMT ($k \rightarrow 0^+$), and the Calogero-Moser model ($k = 2$). We have shown that the underlying effective field theory that determines the average density profile for large N is governed by fundamentally different physics for $-2 < k < 1$ and $k > 1$. In the former case, the large distance behavior of the interaction potential dominates, while the latter case is governed by its short distance behavior. It would be interesting to study other observables beyond the average density for general $k > -2$. For instance, for the Dyson’s log gas ($k \rightarrow 0^+$) the position of the rightmost particle x_{\max} (the largest eigenvalue of a random matrix), centered and scaled, is known to converge to the celebrated Tracy-Widom distribution [59]. The corresponding extreme value distribution for $k = -1$ has recently been computed exactly [9,10] and the case $k = 2$ has been recently computed numerically [32]. It would be interesting to compute the limiting distribution of x_{\max} for generic $k > -2$. Finally, it would be interesting to see if our predictions for the average density can be measured in cold atom experiments. From that perspective, it would be nice to extend our results for the density profile to higher dimensions.

We thank T. Leblé, E. Saff, and S. Serfaty for pointing out useful references and O. Zeitouni for stimulating discussions. M.K. acknowledges support from Grant No. 6004-1 of the Indo-French Centre for the Promotion of Advanced Research (IFCPAR), the Ramanujan fellowship Grant No. SB/S2/RJN-114/2016, and the SERB Early Career Research Grant No. ECR/2018/002085 from the Science and Engineering Research Board (SERB), Department of Science and Technology, Government of India. A.D., A.K., S.N.M., and G.S. acknowledge support from Grant No. 5604-2 of the Indo-French Centre for the Promotion of Advanced Research (IFCPAR). This work was supported by a research grant from the Center for Scientific Excellence at the Weizmann Institute of Science. A.D., A.K., S.N.M., and G.S. acknowledge the hospitality of the Weizmann Institute during the SRITP workshop “Correlations, fluctuations, and anomalous transport in systems far from thermal equilibrium” held at the Weizmann Institute. S.N.M. acknowledges the hospitality of the Weizmann Institute during a visit as a Weston Professor and the support from

the Science and Engineering Research Board (SERB, government of India), under the VAJRA faculty scheme (Grant No. VJR/2017/000110) during a visit to Raman Research Institute, where part of this work was carried out. We thank the ICTS program “Universality in random structures: Interfaces, matrices, sandpiles” (Grant No. ICTS/URS2019/01) for enabling valuable discussions with many participants. A.K. acknowledges support from DST Grant No. ECR/2017/000634.

Note added in proof.—Recently, we came to know from O. Zeitouni that the case $k > 1$ was also studied in the mathematics literature [60].

-
- [1] M. Riesz, *Acta Sci. Math. Univ. Szeged* **9**, 1 (1938).
 - [2] N. S. Landkof, *Foundations of Modern Potential Theory* (Springer, New York, 1972), Vol. 180.
 - [3] D. Chafaï, N. Gozlan, and P. A. Zitt, *Ann. Appl. Probab.* **24**, 2371 (2014).
 - [4] T. Leblé and S. Serfaty, *Inventiones Mathematicae* **210**, 645 (2017).
 - [5] P. J. Forrester, *Log-Gases and Random Matrices* (Princeton University Press, Princeton, NJ, 2010).
 - [6] A. Lenard, *J. Math. Phys. (N.Y.)* **2**, 682 (1961).
 - [7] S. Prager, *Adv. Chem. Phys.* **4**, 201 (1962).
 - [8] R. J. Baxter, *Proc. Cambridge Philos. Soc.* **59**, 779 (1963).
 - [9] A. Dhar, A. Kundu, S. N. Majumdar, S. Sabhapandit, and G. Schehr, *Phys. Rev. Lett.* **119**, 060601 (2017).
 - [10] A. Dhar, A. Kundu, S. N. Majumdar, S. Sabhapandit, and G. Schehr, *J. Phys. A* **51**, 295001 (2018).
 - [11] F. D. Cunden, P. Facchi, M. Ligabò, and P. Vivo, *J. Stat. Mech.* (2017) P053303.
 - [12] F. J. Dyson, *J. Math. Phys.* **3**, 140 (1962); **3**, 157 (1962); **3**, 166 (1962).
 - [13] M. L. Mehta, *Random Matrices* (Academic Press, Amsterdam, 2004).
 - [14] *The Oxford Handbook of Random Matrix Theory* edited by G. Akemann, G. Baik, and P. Di Francesco (Oxford University Press, Oxford, UK, 2011).
 - [15] G. Livan, M. Novaes, and P. Vivo, *Introduction to Random Matrices—Theory and Practice* (Springer, New York, 2018).
 - [16] I. Dumitriu and A. Edelman, *J. Math. Phys. (N.Y.)* **43**, 5830 (2002).
 - [17] E. P. Wigner, *Proc. Cambridge Philos. Soc.* **47**, 790 (1951).
 - [18] M. Prähofer and H. Spohn, *Phys. Rev. Lett.* **84**, 4882 (2000); M. Prähofer and H. Spohn, *J. Stat. Phys.* **108**, 1071 (2002).
 - [19] R. Marino, S. N. Majumdar, G. Schehr, and P. Vivo, *Phys. Rev. Lett.* **112**, 254101 (2014).
 - [20] D. S. Dean, P. Le Doussal, S. N. Majumdar, and G. Schehr, *Phys. Rev. A* **94**, 063622 (2016).
 - [21] D. S. Dean, P. Le Doussal, S. N. Majumdar, and G. Schehr, *J. Phys. A* **52**, 144006 (2019).
 - [22] Y. Castin, in *Ultra-cold Fermi Gases*, edited by M. Inguscio, W. Ketterle, and C. Salomon (IOS Press, Amsterdam, 2006).
 - [23] M. E. Fisher, *J. Stat. Phys.* **34**, 667 (1984).

- [24] G. Schehr, S. N. Majumdar, A. Comtet, and J. Randon-Furling, *Phys. Rev. Lett.* **101**, 150601 (2008).
- [25] J. Bun, J.-P. Bouchaud, S. N. Majumdar, and M. Potters, *Phys. Rev. Lett.* **113**, 070201 (2014).
- [26] F. Calogero, *J. Math. Phys. (N.Y.)* **10**, 2197 (1969).
- [27] F. Calogero, *J. Math. Phys. (N.Y.)* **12**, 419 (1971).
- [28] F. Calogero, *Lett. Nuovo Cimento* **13**, 411 (1975).
- [29] J. Moser, in *Surveys in Applied Mathematics* (Elsevier, New York, 1976), pp. 235–258.
- [30] A. P. Polychronakos, *J. Phys. A* **39**, 12793 (2006).
- [31] F. Calogero, *J. Math. Phys.* **22**, 919 (1981).
- [32] S. Agarwal, M. Kulkarni, and A. Dhar, *J. Stat. Phys.* (2019).
- [33] M. Lu, N. Q. Burdick, S. H. Youn, and B. L. Lev, *Phys. Rev. Lett.* **107**, 190401 (2011).
- [34] A. Griesmaier, J. Werner, S. Hensler, J. Stuhler, and T. Pfau, *Phys. Rev. Lett.* **94**, 160401 (2005).
- [35] K.-K. Ni, S. Ospelkaus, D. Wang, G. Quémener, B. Neyenhuis, M. De Miranda, J. Bohn, J. Ye, and D. Jin, *Nature (London)* **464**, 1324 (2010).
- [36] F. D. Cunden, P. Facchi, M. Ligabò, and P. Vivo, *J. Phys. A* **51**, 35LT01 (2018).
- [37] J. M. Brown and A. Carrington, *Rotational Spectroscopy of Diatomic Molecules* (Cambridge University Press, Cambridge, England, 2003).
- [38] These results are valid at sufficiently low temperature, i.e., for $\beta \gg N^{-2\alpha_k}$, where α_k is given in Eq. (4). For $\beta = O(N^{-2\alpha_k})$, it is no longer sufficient to minimise just the energy and one has to take into account the contributions from the entropy, which will modify the average density. The relative importance of the energy and the entropy terms has been discussed in several previous works, see e.g., [39–41]. The entropy modified density was computed explicitly for the log-gas, i.e., in the $k \rightarrow 0^+$ limit [42], and also for the eigenvalue density of the Wishart-Laguerre matrices [43]. For another interesting recent application in the context of generalized hydrodynamics see Ref. [44].
- [39] M. K. H. Kiessling and H. Spohn, *Commun. Math. Phys.* **199**, 683 (1999).
- [40] F. D. Cunden, P. Facchi, and P. Vivo, *J. Phys. A* **49**, 135202 (2016).
- [41] F. D. Cunden, P. Facchi, M. Ligabò, and P. Vivo, *J. Stat. Phys.* **175**, 1262 (2019).
- [42] R. Allez, J.-P. Bouchaud, and A. Guionnet, *Phys. Rev. Lett.* **109**, 094102 (2012).
- [43] R. Allez, J. P. Bouchaud, S. N. Majumdar, and P. Vivo, *J. Phys. A* **46**, 015001 (2013).
- [44] H. Spohn, arXiv:1902.07751.
- [45] See Supplemental Material at <http://link.aps.org/supplemental/10.1103/PhysRevLett.123.100603>, which includes Refs. [46,47], for more details on the computations.
- [46] F. G. Tricomi, *Integral Equations* (Dover Publications, New York, 1985).
- [47] S. N. Majumdar and G. Schehr, *J. Stat. Mech.* (2014) P01012.
- [48] D. S. Dean and S. N. Majumdar, *Phys. Rev. Lett.* **97**, 160201 (2006).
- [49] D. S. Dean and S. N. Majumdar, *Phys. Rev. E* **77**, 041108 (2008).
- [50] E. B. Saff and V. Totik, *Logarithmic Potentials with External Fields* (Springer Science & Business Media, Berlin, Heidelberg, 2013), Vol. 316.
- [51] S. Serfaty, *Coulomb Gases and Ginzburg-Landau Vortices*, Zurich Lectures in Advanced Mathematics (European Mathematical Society (EMS), Zürich, 2015).
- [52] N. Ya Sonin, *Studies of Cylinder Functions and Special Polynomials* (Gostekhizdat, Moscow, 1954) (in Russian).
- [53] G. Y. Popov, *The Elastic Stress' Concentration around Dies, Cuts, Thin Inclusions and Reinforcements* (Nauka, Moscow, 1982).
- [54] H. Widom, *J. Stat. Phys.* **94**, 347 (1999).
- [55] S. V. Buldyrev, M. Gitterman, S. Havlin, A. Ya. Kazakov, M. G. E. da Luz, E. P. Raposo, H. E. Stanley, and G. M. Viswanathan, *Physica (Amsterdam)* **302A**, 148 (2001); *Phys. Rev. E* **64**, 041108 (2001).
- [56] B. Derrida, *J. Stat. Mech.* (2007) P07023.
- [57] J. Cividini, A. Kundu, A. Miron, and D. Mukamel, *J. Stat. Mech.* (2017) P013203.
- [58] A. Miron, *Phys. Rev. E* **100**, 012106 (2019).
- [59] C. A. Tracy and H. Widom, *Commun. Math. Phys.* **159**, 151 (1994); C. A. Tracy and H. Widom, *Commun. Math. Phys.* **177**, 727 (1996).
- [60] D. P. Hardin, T. Leblé, E. B. Saff, and S. Serfaty, *Constr. Approx.* **48**, 61 (2018).